Influence of Organic Fouling Layer Characteristics and Osmotic Backwashing Conditions on Cleaning Efficiency of RO Membranes

Influence of Organic Fouling Layer Characteristics and Osmotic Backwashing Conditions on Cleaning Efficiency of RO Membranes

Sorcha Daly[c], Ashley Allen[a], Vasileios Koutsos[b], Andrea J.C. Semião[a]*

To be submitted to

Journal of Membrane Science

[a] Institute for Infrastructure and Environment, School of Engineering, The University of Edinburgh, William Rankine Building, The King's Buildings, Thomas Bayes Road, Edinburgh, EH9 3FG, United Kingdom

[b] Institute for Materials and Processes, School of Engineering, The University of Edinburgh, Sanderson Building, The King's Buildings, Robert Stevenson Road, Edinburgh, EH9 3FB, United Kingdom

[c] Formerly Institute for Infrastructure and Environment, School of Engineering, University of Edinburgh. Currently School of Chemical and Bioprocess Engineering, University College Dublin (UCD), Belfield, Dublin 4, Ireland

[*]Corresponding author: Dr Andrea J.C. Semião, Andrea.Semiao@ed.ac.uk

Keywords: reverse osmosis, fouling, osmotic backwashing, calcium

Abstract

Fouling remains a prevalent and serious problem in industries using membrane processes. Efforts to mitigate fouling are improving, however, membrane fouling cannot be completely eliminated. Therefore fouling control via development of sustainable cleaning methods are crucial. Despite osmotic backwashing showing promise, little is understood about this cleaning method for removal of fouling from reverse osmosis (RO) membranes. This paper systematically examines how organic fouling characteristics and osmotic backwashing parameters influence cleaning efficiency. Alginic acid was used as a model foulant and numerous microscopy techniques, including confocal microscopy, scanning electron microscopy and atomic force microscopy were used to examine the membrane fouling before and after cleaning to gain a clearer understanding of the mechanisms involved. Increasing $CaCl_2$ concentration in the fouling solution resulted in an increase in fouling layer thickness from 37 to 179 μm, due to the complexation of Ca^{2+} and the carboxyl groups in the alginate. Osmotic backwashing efficiency with 0.7 M NaCl decreased as the fouling layer became thicker and the pure water flux (PWF) recovery decreased from 92% to 81%. Osmotic backwashing efficiency also decreased with increasing initial permeate flux, as less fouling was removed: the fouling generated at higher initial fluxes is largely irreversible, resulting in a denser and more compact fouling layer. In an effort to increase osmotic backwashing flux, a $CaCl_2$ draw solution was used, however, the Ca^{2+} ions were found to interact with the alginate in the fouling layer, rendering this method inefficient, when compared to NaCl draw solutions which originated similar osmotic backwashing fluxes. Interestingly, the fouling layer was found to swell from 16 μm to 141 μm, when osmotic backwashing was carried out with a NaCl draw solution, followed by contact with a low ionic strength solution used for PWF testing. This phenomenon does not occur to the same extent after backwashing with $CaCl_2$. The same trends were obtained for bovine serum albumin (BSA) fouling, whilst humic acid (HA) did not display any swelling phenomena. However, it showed the same cleaning inefficiency when using $CaCl_2$ as a draw solution.

1. Introduction

By 2025, 60% of the world's population will live in water stressed areas [1]. As seawater is the Earth's most abundant resource, seawater desalination can offer a solution to this urgent water crisis. Membrane technology is now the most widely applied water purification process for desalination and other water reclamation processes [2], with installed capacity having more than doubled in the last 15 years [3]. The particular use of reverse osmosis (RO) in seawater desalination for potable water production represents 60% of the installed desalination membrane process capacity. However, this technology suffers drawbacks, most notably membrane fouling. Membrane replacements and chemicals alone, can represent at least 22% of the cost of producing water with RO [3, 4].

Membrane fouling leads to permeability losses and, therefore, drives up costs in RO desalination. Organic fouling is amongst the many potential foulants that are widespread in natural waters and wastewaters, with seawater RO plants being mainly fouled by organic material [5]. Organic fouling in RO processes has been widely reported in the literature [6-9]. Lee and Elimelech [10] studied alginate fouling and found that in the presence of 1 mM $CaCl_2$, the permeate flux declined by 65%. Similarly, Tang et al. [6] fouled RO membranes with humic acid, also reporting 65% flux decline in the presence of 1 mM $CaCl_2$, as opposed to less than 10% in the absence of $CaCl_2$. Furthermore, fouling has also been shown to affect rejection by RO membranes because of cake enhanced concentration polarization [11]. Due to the nature of filtration, fouling is unavoidable and therefore effective and sustainable cleaning strategies should be a fundamental part of membrane processes.

Various cleaning methods have been tested as a way to mitigate membrane fouling, with varying results being reported. The current most prevalent form of cleaning is chemical cleaning. Ang et al. [12] used numerous combinations of chemicals in RO membranes treating wastewater effluent from a municipal treatment plant. A combination of ethylenediaminetetraacetic acid (EDTA) and NaOH restored 93% of the pure water flux (PWF). In a similar study, fouling with sodium alginate, Suwannee River natural organic matter, bovine serum albumin, and octanoic acid was carried out in the presence of 0.5 mM Ca^{2+} [13]. Cleaning with 0.5 mM EDTA at pH 11 restored 91% of the PWF. Albeit with good recoveries, these cleaning methods are not 100% efficient and the chemical agents used are known to be harmful to the environment [14]. Furthermore, chemical cleaning can damage the membrane, hence affecting its performance and longevity. Simon et al. [15] chlorinated

polyamide NF/RO membranes, affecting the membrane permeability and trace contaminant rejection. Klüpfel et al. [16] examined NF micropollutant rejection after cleaning with NaOH, and a decrease in clofibric acid and metamitron rejections from 100% to less than 80% and from 60% to 20% were, respectively, obtained. The use of these chemicals should therefore be limited and chemical free cleaning methods for RO membranes should be explored.

Some work has been performed on chemical free cleaning in RO with widely varying results [17-20]. Physical cleaning experiments by increasing the crossflow velocity were performed by Lee et al. [18]. This cleaning method was unsuccessful in restoring the flux of RO membranes fouled with alginic acid in the presence of Ca^{2+}, for example. This was caused by the compact and dense structure of the fouling layer due to the hydraulic pressure applied during fouling. No further attempts were made to restore the RO flux in this study. Ramon et al. [19] also found that cleaning with deionised water was ineffective in restoring the flux after organic fouling of RO membranes. In contrast, Tow et al. [20] used deionised water cleaning and restored over 70% of the flux after organic fouling in RO. More work is needed to fully understand chemical free cleaning in RO, in order to optimise it.

Physical cleaning by osmotic backwashing has been suggested as a way to clean RO membranes more efficiently [17, 19-21]. Osmotic backwashing reverses the permeate flux direction from the permeate side to the feed side, and can be implemented in different ways, including reducing the applied pressure (e.g. down to ambient pressure) or by injecting a pulse of high salt concentration on the feed side, i.e. by introducing a draw solution: the osmotic pressure difference between the feed and permeate sides overcomes the applied hydraulic pressure and the permeate flux is reversed. This reverse in flux direction can potentially remove the fouling layer that has accumulated on the membrane surface. Bar-Zee et al. [17], for example, used osmotic backwashing for biofilm removal from RO membranes and achieved a 63% recovery. Qin et al. [21, 22] have tested this cleaning method for spiral wound RO membranes at pilot scale, showing very promising results: up to 5 kg of fouling debris were removed from each of the membrane modules tested, for example.

A wide range in osmotic backwashing duration has been adopted in the literature, from an injection lasting 50 to 60 seconds [17], to 10 minutes [19], and even up to 1 hour [23]. The cleaning duration should be optimized, as after a certain amount of cleaning time, osmotic backwashing flux ceases [24-27]. Furthermore, cleaning duration should be maintained as short

as possible in order to reduce time lost due to cleaning, as well as reduce the amount of osmotic backwashing solution needed, but always ensuring cleaning efficiency.

Ramon, Nguyen et al. [19] examined the use of osmotic backwashing to clean RO membranes fouled with alginic acid. Osmotic backwashing with a 10 minute pulse of 96 $g.L^{-1}$ NaCl restored 93% of the PWF and outperformed physical cleaning with deionized water by shearing with crossflow, which only restored 66% of the PWF. The addition of NaOH increased the osmotic backwashing efficiency to 97%. Tow et al. [20] also fouled RO membranes with alginic acid and 1 mM $CaCl_2$, followed by cleaning with increase in crossflow velocity and/or osmotic backwashing, by reducing the applied pressure. This cleaning method restored 80% of the PWF. However, no further attempts were made in these studies to optimise osmotic backwashing or study how different fouling and osmotic backwashing characteristics affect cleaning efficiency. Furthermore, no surface imaging techniques were used to visualize and quantify the remaining fouling on the membrane surface, which is an important indicator of cleaning efficiency [28]. In previous osmotic backwashing studies, cleaning efficiencies of over 90% have been achieved [19, 23], while for other studies, osmotic backwashing was not as effective, with less than 80% PWF recovery [13, 17, 20].

There is a clear lack of understanding if and how fouling layer characteristics affect osmotic backwashing, and how osmotic backwashing characteristics affect the cleaning efficiency, hence inviting further studies on this promising cleaning technique. Boo et al. [29] showed that fouling characteristics by silica nanoparticles impacted on cleaning efficiency of forward osmosis membranes. Cleaning was carried out by increasing the cross-flow velocity by a factor of three, which allowed for 95% recovery of initial flux of membranes fouled at pH 4. However, when the membranes were fouled at pH 9, the same cleaning method only restored 80% of the initial flux. This was caused by increased silica nanoparticle aggregation, which destabilize at higher pH, consequently forming a thicker and less porous fouling layer, making it more challenging to remove. Ang et al. [30] studied how organic fouling composition can affect cleaning efficiency in RO. They examined the cleaning efficiency of RO membranes fouled with alginate, Suwannee River natural organic matter (SRNOM) and combinations of both, using 0.5 mM ETDA. Cleaning was 100% efficient for 20 mg/L SRNOM fouling. However, as alginate was added to the fouling solution and the concentration increased, the cleaning efficiency decreased down to 45% for fouling with 20 mg/L alginate. In a separate study, Ang et al. [13] also examined the cleaning efficiency of different cleaning chemicals, namely deionised water, NaOH and 0.5 mM EDTA, on different fouling mixtures of alginate,

SRNOM, BSA and octanoic acid. In contrast to the previous study [30], each cleaning solution became more efficient when the alginate concentration was increased 3 fold. This leads to hypothesizing that osmotic backwashing will also be highly dependent on the fouling characteristics, where the latter can be affected by many factors. Solution chemistry, such as the presence of Ca^{2+} in the feed, and operating pressure, i.e. initial permeate flux, have already been shown to greatly influence the rate and extent of fouling [6, 10, 31], but no work has shown how these parameters affect osmotic backwashing. Furthermore, as the chemistry of the feed solution has a significant influence on the fouling layer characteristics, it is questioned whether the osmotic backwashing solution chemistry could alter the fouling layer during osmotic backwashing, as was shown for FO [28]. However, as the fouling characteristics are very different between RO and FO [18, 32, 33] due to the different driving forces involved, this needs to be checked for RO.

The aim of this study is to examine the efficiency of osmotic backwashing as a way of removing organic fouling from RO membranes through both flux measurements and surface imaging. As limited information is provided in the literature on fouling layer properties before and after osmotic backwashing, several surface imaging techniques were performed in this study to obtain an improved understanding of the fouling layer structure. Confocal microscopy is used to determine the thickness of the fouling layer before and after osmotic backwashing. Atomic force microscopy is used to quantify the adhesion forces and elasticity of the fouling layers. SEM is also used to examine the fouling layer morphology both before and after backwashing.

2. Materials and Methods

2.1 Reverse osmosis membrane: BW30

A commercial flat sheet reverse osmosis membrane BW30 (Dow Filmtec^{TM}) was used for all experiments in this study. The BW30 membrane is a thin film composite (TFC) membrane with aromatic polyamide active layer on a polysulphone intermediate support layer. The membranes were stored dry at room temperature. They were cut to fit the membrane cells and stored in MilliQ water overnight at 4ºC before use. Prior to use the membranes were gently rinsed with MilliQ water. The membrane pure water permeability was 3.94 ± 0.21 $L.h^{-1}.m^{-2}.bar^{-1}$, corresponding to a membrane resistance of 1.71×10^{12} m^{-1}.

2.2 Organic Fouling Feed Solutions

The main organic fouling feed solution contained alginic acid sodium salt (AA) derived from brown algae (Sigma Aldrich, UK). AA was chosen as a model foulant for polysaccharides found in wastewater [34], as well as polysaccharides excreted by Pseudomonas bacteria during biofilm formation [35]. Furthermore, AA was also chosen due to its suitability for use with confocal imaging microscopy. To further examine the effect of osmotic backwashing ions on the fouling layer of other types of organic matter, fouling was also carried out using humic acid (HA) and bovine serum albumin (BSA) for comparison (Sigma Aldrich, UK).

The fouling solutions of each foulant were made from a stock concentration of 2 $g.L^{-1}$. The stock solution was stirred overnight to ensure the foulant was fully dissolved. A feed solution of 60 $mgC.L^{-1}$ foulant in MilliQ water was used with a buffer and background electrolyte solution of 1 mM $NaHCO_3$ (Sigma-Aldrich, UK), 20 mM NaCl (Fisher Scientific, UK) and $CaCl_2$ (Sigma-Aldrich, UK). The concentration of $CaCl_2$ depended on the experiment. These fouling solutions were selected to accelerate and promote irreversible fouling [32, 36, 37].

2.3 Reverse Osmosis Crossflow System

Figure 1 illustrates the custom built stainless steel RO crossflow system used in this study. A diaphragm pump (P200 Hydra-Cell, UK) delivered constant flow to two stainless steel membrane cells (MMS, Switzerland) from 3 reservoirs. The three reservoirs were designated for the fouling feed solution, the osmotic backwashing solution and MilliQ water. Each cell had an effective membrane area was of 0.0048 m^2 (membrane width of 25 mm and length of 191 mm) and a feed channel height of 1 mm.

The inlet flow was fitted with a flowmeter (M2SSPI Hydrasun, UK), a pressure transducer (S model, Swagelok) and a thermocouple (WTM Pt 100-0-6 Condustrie-Met Ag, Germany) to monitor flow conditions. The temperature of the feed tank was maintained at 20 ± 1°C by a cooling bath (Haake F3, UK) with a submerged coil. Each tank contained one conductivity meter (Cond 340i meter, WTW, Germany) for monitoring purposes, and pH was also measured during the experiments. The feed solution pH was of 7.2 ± 0.7. The temperature, pressure and flowrate were logged with a DAQ 55 Omega data logger (Omega, UK). A back-

pressure regulator (Swagelok, UK) was used to vary the pressure applied to the membrane. A pressure relief valve (Swagelok, UK) was fitted for safety.

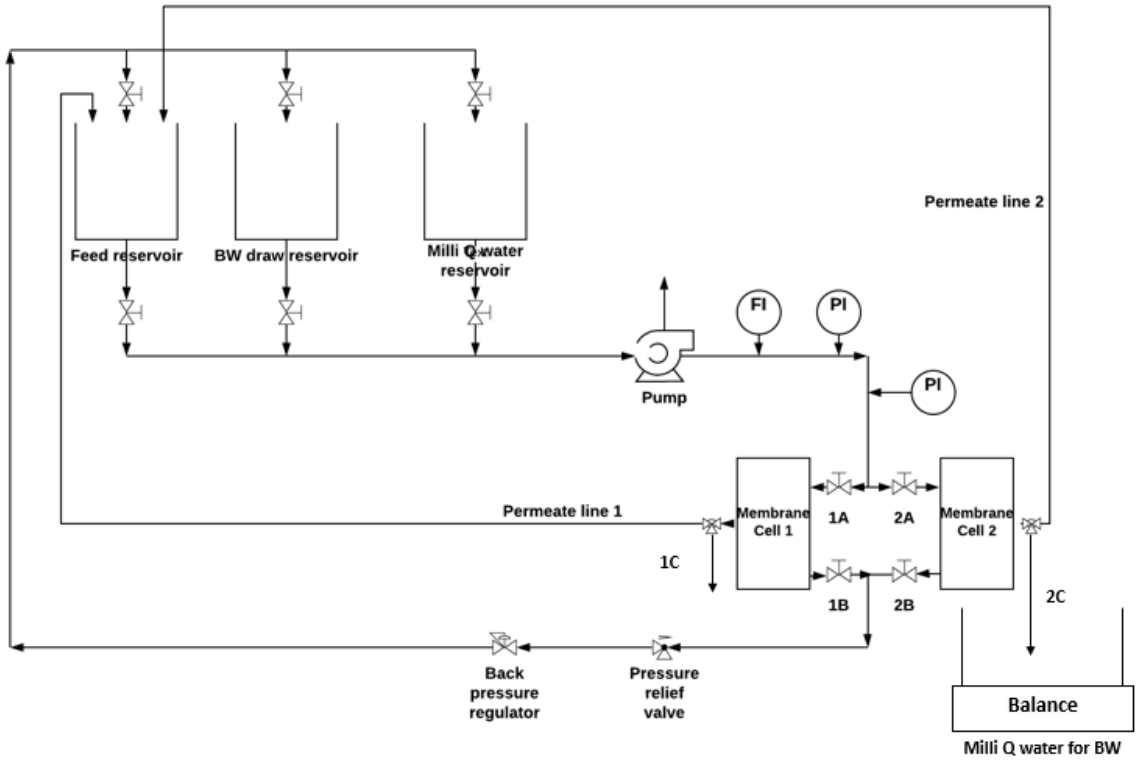

Figure 1 - P&ID of the RO crossflow system

The crossflow was maintained at 0.9 $L.min^{-1}.cell^{-1}$. To ensure the flow was split evenly between the two cells, one pressure transducer was placed on each cell. Calculations showed that the pressure in both cells were within 3% of each other, hence showing that the flow divided evenly to produce accurate results. Furthermore, fouling with 60 mgC/L alginic acid at 20 bar was performed on both cells simultaneously with fouling layer thicknesses determined to be 53.2 ± 9.3 µm and 52.9 ± 8.7 µm for membranes in cell 1 and 2, respectively, again showing that the flow divided evenly between the cells.

2.4 Fouling Protocol

The membranes were compacted overnight for at least 18 hours at 25 bar using MilliQ ultrapure water (Avidity, UK). For the particular case of the experiment with an initial flux of 100 $L.h^{-1}.m^{-2}$ and 30 bar, the membrane was compacted at 32 bar. Once the membrane was compacted, the PWF was measured with MilliQ water for 30 minutes at 20 bar, to ensure the pure water flux was constant.

The permeate was collected from a valve 1C and 2C on the permeate line over a known amount of time and weighed on a balance (Ohaus, UK). Next, the system was stabilised for 30 minutes with the buffer and background electrolyte solution (described in section 2.2) at the required initial permeate flux, when the flux was recorded. The applied pressure depended on the required initial permeate flux of each experiment, which unless otherwise stated, was set to 20 bar for an initial permeate flux of 80 $L.m^{-2}.h^{-1}$, in order to accelerate fouling. Next, the foulant was added to the feed solution and fouling was carried out for 6.5 hours in total recirculation mode. The flux was determined at 20 minute intervals for the first hour of fouling and then every hour for the remainder of the experiment. Permeate flux was calculated as follows:

$$J_v = \frac{1}{A}\frac{dV}{dt} \qquad (1)$$

where J_v is the permeate flux ($L.h^{-1}.\ m^{-2}$), A is the membrane area (m^2), V is the volume of water (L) collected on the balance for a certain period of time, and t is the time of collection (h).

2.5 Osmotic Backwashing Cleaning Protocol

Membrane surface cleaning by osmotic backwashing was carried out immediately after fouling. After fouling, the applied hydraulic pressure was reduced to ambient pressure in the system (i.e. 1.2-1.5 bar) and the recirculation pump was stopped. Then, cell 1 was isolated from the system by closing the inlet and outlet valves (i.e. valves 1A, 1B and 1C in Figure 1). Valve 2C for cell 2 was turned to change from total recirculation mode used during fouling to permeate collection mode, whilst feed and retentate were still under recirculation mode. Osmotic backwashing was then implemented in cell 2 by inserting a high salinity pulse draw solution in the feed channel for 1 minute at a flowrate of 0.9 $L.min^{-1}$. A cleaning time of 1 minute was chosen because the osmotic backwashing flux was found to reduce by 50% after 2 minutes, and reducing to zero after 3 minutes: this is due to a lack of 100% retention capability by the membrane and occurrence of internal concentration polarization during osmotic backwashing. The osmotic backwashing draw solution used was 0.7 M NaCl, unless otherwise specified, in order to mimic seawater. The osmotic backwashing flux was determined by weighing the weight loss of the permeate solution in the MilliQ water for BW reservoir, which was placed in a balance (Ohaus, UK). The natural process of osmosis was hence used. After

osmotic backwashing, the PWF was retested at 20 bar for 30 minutes. For some particular experiments, the PWF was not measured after osmotic backwashing in order to determine if this measurements affected the fouling layer.

The membranes were carefully removed from the cross-flow cells to carry out microscopy visualisation techniques. The entire crossflow system including the empty cells were thoroughly cleaned, firstly by rinsing with MilliQ water, followed by recirculation of 0.1 M NaOH for 30 minutes. The NaOH solution was then neutralised with 0.1 M HCl. The system was thoroughly rinsed with MilliQ water until the conductivity was <1 $\mu S.cm^{-1}$ and pH was neutral, measured with a pH probe (VWR, Germany).

2.6 Sample Staining

To determine osmotic backwashing efficiency, concanavalin A (Con A) dye was used to stain the fouled membrane and the osmotically backwashed membrane. Con A Alexa Fluor™ 488 Conjugate (ThermoFisher Scientific), displaying bright green fluorescence was used in this study. The lectin Con A binds to mannose residues of glycoproteins and is a widely used dye to stain polysaccharides like alginic acid. Stock solutions of 1 $mg.ml^{-1}$ of Con A were prepared and frozen in 0.1 ml volumes.

At least three 20 × 20 mm^2 membrane samples were cut from the centre of the fouled membrane. The samples were then placed on a glass slide, and 50 µl of thawed Con A solution was applied directly on the fouling layer using a micropipette. These samples were incubated for 30 minutes in the dark. Double sided tape was used to make an adapted washer, which was placed around the sample to act as an O-ring, followed by a glass coverslip which was placed on top of the O-ring. The O-ring, positioned between the glass slide and the coverslip, was used to stop the coverslip from compressing the gel fouling layer and causing inaccurate results.

2.7 Confocal Laser Scanning Microscopy (CLSM)

A Zeiss LSM 880 with Fast Airyscan CLSM, and with a laser scanning module fitted on an inverted microscope (Zeiss) and an argon laser, was used to image 3 different areas of each membrane sample. Images were recorded with an excitation wavelength of 488 nm and generated by obtaining Z-stacks of the fouling layer. This microscope has lateral resolution of

200 nm for 2D and 3D Z stacks and 500 to 600 nm axial resolution for Z-stacks. The lowest increment quantified by the microscope is < 25 nm. Imaris^{TM} software was used for image analysis, in order to accurately see and quantify the fouling layer thickness. The heterogeneity of the fouling layer was not considered in this study, since it was found that the surface coverage of the membrane by the fouling layer was uniform. The membrane emitted some background fluorescence and therefore its thickness was determined based on several measurements and was determined to be 33 ± 2.5 μm. This membrane thickness was subtracted from the fouling layer thickness values obtained by the microscope to determine the net fouling layer thickness.

2.8 Cryo Scanning Electron Microscopy (Cryo SEM)

Cryo SEM was used to visualise and compare the surface morphology of the fouled and osmotically backwashed membranes. A Hitachi S4700 Scanning Electron Microscope equipped with an 8k x 8k CMOS sensor was used. First the wet samples were mounted on a metal stub and "cryo-fixed" by submerging them into sub-cooled nitrogen (nitrogen slush) at -210^{o}C using a controlled environment freezing apparatus (VitrobotTM). The stub containing the samples was immediately moved to the cold-stage of the SEM cryo-preparation chamber, and placed under vacuum. The samples were then sputter coated with gold and transferred into the SEM chamber for imaging. Each sample was mounted onto the same metal stub together at the same time to ensure they experienced identical cryo-fixing and sputter coating conditions ensuring the results were reliable and correct for each sample. This allows visualizing the sample without the need to dry it, hence preserving its properties.

2.9 Scanning Electron Microscopy (Energy Dispersive X-Ray Spectroscopy)

Scanning Electron Microscopy / Energy Dispersive X-Ray Spectroscopy (SEM-EDS) was used to perform elemental analysis of the fouled and osmotically backwashed membranes and to map the membrane surfaces to determine the distribution of elements on the surface, especially Ca^{2+}. A Carl Zeiss SIGMA HD VP Field Emission SEM and Oxford AZtec ED X-ray analysis software was used. The membrane samples were allowed to dry overnight, being subsequently coated with carbon overnight, before being placed under vacuum in the SEM.

Maps and spectra were recorded using an accelerating voltage of 10 kV, an aperture size of 80 μm, and a working distance of 7 ± 1 mm.

2.10 Atomic Force Microscopy

The apparent Young's modulus (elastic modulus) and adhesive force of the fouled and backwashed membranes were determined by examining indentation and retraction curves obtained using atomic force microscopy (AFM). Force measurements were performed using the MFP-1D (Asylum Research, Santa Barbara, CA, USA). The MFP-1D is mounted on an inverted optical microscope (Nikon TE2000-U, Nikon UK Limited, Surrey, UK) and attached to a digital camera (Orca – ER C4742-80, Hamamatsu Photonics, Japan). A commercial silicon nitride cantilever with a sharp triangular silicon nitride tip of 60 nm radius (DNP-10, C type, Bruker, UK) with a spring constant of 0.142 N/m was used in this study. The raw data was analysed using the Hertz model fitting with PUNIAS software with a constant Poisson ratio of 0.5. At least 50 measurements of each sample were taken to get average measurements.

3. Results and Discussion

3.1 Influence of feed solution chemistry on osmotic backwashing efficiency

The presence of Ca^{2+} in the AA fouling solution has a significant effect on the rate and extent of RO fouling [6, 10]. Carboxylic groups present in AA form complexes with Ca^{2+}, known as the "egg box model", neutralizing the negative charge of alginate molecules, resulting in a thick compact gel fouling layer on the surface of the membrane [38, 39]. Lee and Elimelech [10] reported a 75% increase in flux reduction when RO membranes were fouled with AA in the presence of 1 mM Ca^{2+} compared to the absence of Ca^{2+}. This influence of fouling on membrane performance is expected to have an influence as well on cleaning efficiency using osmotic backwashing. However, to what extent is not yet known. In order to examine how feed solution chemistry during fouling affects cleaning efficiency, osmotic backwashing was applied to BW30 membranes fouled under various solution chemistries by varying Ca^{2+} concentration.

As can be seen in Table 1, an increase in Ca^{2+} concentration in the feed from 0 to 2.5 mM causes an increase in permeate flux decline from 10% up to 69%, respectively. Lee and Elimelech also demonstrated significant flux reductions during organic fouling upon the

addition of Ca^{2+} ions [10]. Hong and Elimelech [38] and Li and Elimelech [39] also reported pronounced permeate flux reductions of 39% and 50%, respectively, after the addition of Ca^{2+} in organic fouled nanofiltration membranes, as opposed to 10% in the absence of Ca^{2+}. They explained this is due to the denser and highly compact organic fouling layer formed in the presence of Ca^{2+}, resulting in a higher resistance to flux.

Table 1 - Permeate flux decline (%) and osmotic backwashing flux ($L.h^{-1}.m^{-2}$) as a function of Ca^{2+} concentration (mM) in the feed solution

Ca^{2+} Concentration (mM)	**% Permeate flux decline**	**Osmotic Backwashing flux ($L.h^{-1}.m^{-2}$)**
0	10 ± 0.7	23 ± 3.9
1	57 ± 0.7	26 ± 0.3
2	66 ± 1.4	19 ± 1.4
2.5	69 ± 2.1	16 ± 2.2

The increase in permeate flux decline is accompanied by an increase in the fouling layer characteristics formed on the membrane surface as Ca^{2+} is introduced in the feed. As can be seen in Figure 2, the fouling layer thickness increased from 37 μm in the absence of Ca^{2+} to 238 μm in the presence of 1 mM Ca^{2+}. This is caused by the complexation between Ca^{2+} ions and AA molecules, as previously mentioned, where the thicker fouling layer offered greater resistance to flux and therefore an increase in permeate flux decline occurred. As the concentration of Ca^{2+} increased from 1 to 2 mM, the fouling layer thickness remained relatively unchanged, at 236 μm; yet the flux decline is greater for 2 mM Ca^{2+}, i.e. 66%, as opposed to 57% for 1 mM Ca^{2+}. The fouling layer becomes denser and more cohesive, with further cross linkage of carboxylic groups and Ca^{2+} ions [40]. As the Ca^{2+} concentration increased further to 2.5 mM, the gel layer thickness decreased by 57.3 μm, accompanied by a further flux decline of 69%. This greater resistance to flux, despite the thinner fouling layer, suggests that the layer has become more compact and denser. Moe et al. [41] showed that alginate beads shrink with increase in Ca^{2+} concentration in their surrounding solution.

In order to remove the fouling layer, osmotic backwashing was applied using a draw solution of 0.7 M NaCl. As can be seen in Figure 2 and Table 1, the Ca^{2+} concentration in the fouling feed solution had an influence on the osmotic backwashing efficiency, both in terms of fouling removal and on the osmotic backwashing flux. Osmotic backwashing reduced the fouling layer thicknesses from 37 μm to 31 μm and from 238 μm to 34 μm when the Ca^{2+} concentration in the fouling feed solution increased from 0 mM to 1 mM, respectively. A lack

of complete removal of the fouling layer, even in the absence of Ca^{2+}, can be explained by a high permeate flux used during fouling (i.e. 80 $L.h^{-1}.m^{-2}$ and 23 bar). High permeate fluxes and pressures have been shown to cause the fouling layer to be compact and dense, which is well illustrated when comparing RO fouling layers with FO fouling layers created for the same flux conditions [7, 18]. Foulants subjected to high permeate flux at the beginning of the filtration process will form a denser and more compact fouling layer compared to subsequent foulant deposits, which are subjected to lower permeate flux which declines with time during the experiment. These differences in foulant characteristics were shown through TEM in the study by Tang et al. [7], and have also been shown for biofouling [10]. This will hence make the complete removal of the fouling by osmotic backwashing challenging, especially the cake layer which is closest to the membrane surface.

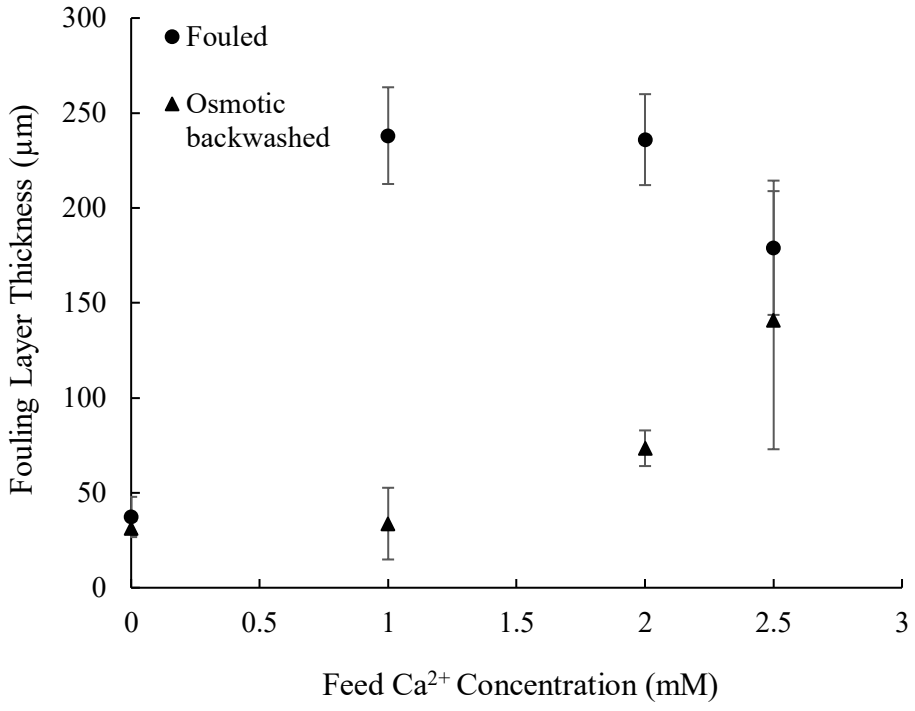

Figure 2 – Fouling thickness before and after osmotic backwashing as a function of feed Ca^{2+} concentration (fouling conditions: FS = 60 $mgC.L^{-1}$ AA, 1 mM $NaHCO_3$, 20 mM NaCl; initial permeate flux = 80 $L.h^{-1}.m^{-2}$; fouling duration = 6.5 hours; osmotic backwashing conditions: duration = 1 minute; DS = 0.7 M NaCl; error bars show standard deviation of repeated experiments)

A further Ca^{2+} concentration increase up to 2.5 mM was accompanied by a reduced cleaning efficiency, where remaining fouling layer thicknesses increased from 34 µm up to 141

μm. Mi and Elimelech [37] and Lee and Elimelech [10] used AFM to show that adhesion forces of the alginate fouling increased up to fourfold with increasing Ca^{2+} concentration up to 1 mM. As the Ca^{2+} concentration increases and the fouling layer becomes more cohesive and compact, osmotic backwashing becomes less efficient in removing it from the membrane. Furthermore, a reduction in the osmotic backwashing flux was also obtained, reducing from 26 to 16 $L.h^{-1}.m^{-2}$ (Table 1), which would contribute to a reduction in the cleaning efficiency. The measurements for pure water flux (PWF) restoration confirm this further. The PWF was restored by 92% for a Ca^{2+} concentration up to 2 mM. However, only 81% of the PWF was restored for the membrane fouled with 2.5 mM Ca^{2+}.

Cleaning efficiency by osmotic backwashing is clearly influenced by the fouling layer characteristics: increasing Ca^{2+} concentrations offers high adhesion to the membrane surface and high cohesion between fouling layers [31], making them more challenging to remove. This is accompanied by a reduction in the osmotic backwashing flux obtained, which reduced cleaning efficiency further. These results also show that a high flux restoration alone cannot confirm significant fouling removal has occurred in RO and highlights the importance of surface imaging to examine true cleaning efficiency. As seen in Figure 2, osmotic backwashing of a fouling layer generated with an initial permeate flux of 80 $L.h^{-1}.m^{-2}$ and a draw solution of 0.7 M NaCl is inefficient in cleaning the membrane for all Ca^{2+} concentrations tested. This suggests that both initial permeate flux and osmotic backwashing flux will influence cleaning efficiency.

3.2 Physical effect of feed solution chemistry on RO fouling and cleaning

Fouling characteristics in NF and RO membranes have been shown to be dependent on the initial permeate flux [7, 38, 40, 42, 43]. Tang et al. [7] obtained thicker and denser humic acid fouling layers on RO membrane surfaces when increasing initial permeate flux. This increase in fouling is therefore expected to impact on osmotic backwashing efficiency. Osmotic backwashing with 0.7 M NaCl as a draw solution was applied to membranes fouled with varying initial permeate fluxes ranging between 20 and 100 $L.h^{-1}.m^{-2}$, with results presented in Figure 3.

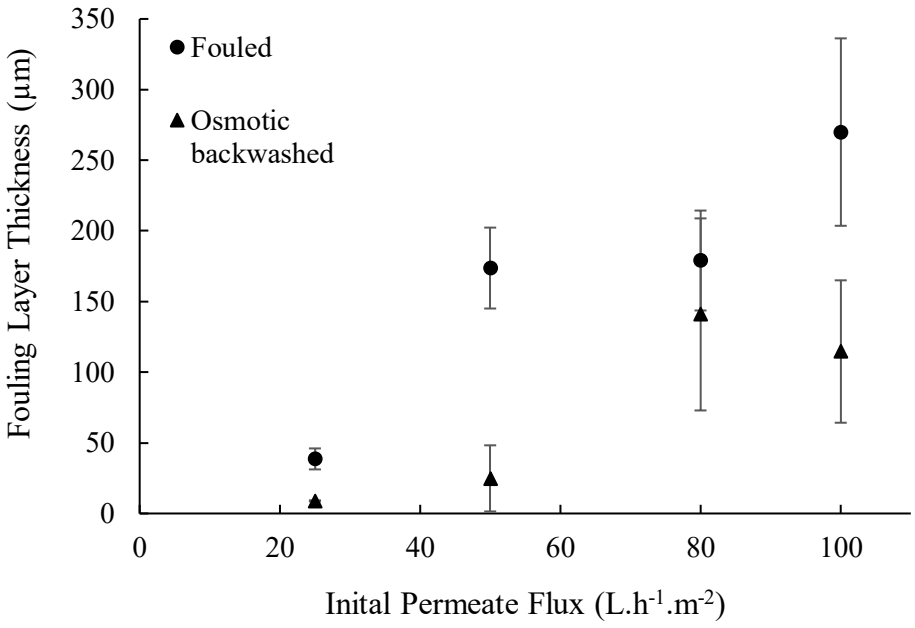

Figure 3 - Fouling thickness before and after osmotic backwashing as a function of initial permeate flux (fouling conditions: FS = 60 mgC.L^{-1} AA, 1 mM $NaHCO_3$, 20 mM NaCl, 2.5 mM $CaCl_2$; fouling duration = 6.5 hours; osmotic backwashing conditions: duration = 1 minute; DS = 0.7 M NaCl; error bars show standard deviation of repeated experiments)

Higher initial permeate fluxes resulted in thicker fouling layers accumulated on the membrane surface, with the layer increasing from 39 µm for an initial permeate flux of 25 L.h^{-1}.m^{-2} to 270 µm for 100 L.h^{-1}.m^{-2}. By increasing the initial permeate flux, and therefore the hydrodynamic drag towards the membrane surface, foulant-membrane and foulant-foulant repulsion forces can be overcome, resulting in significant increased fouling [7, 40, 44]. This is further confirmed by permeate flux decline measurements. As the initial permeate flux increases from 25 to 100 L.h^{-1}.m^{-2}, the permeate flux reduction increases from 19% to 75% (see Table 2). This has been obtained in other studies [40, 45]. Tang et al. [6] showed that initial permeate fluxes of 0.6, 1.2, and 2.2 m.day^{-1} corresponded to flux reductions of 2%, 4%, and 9%, respectively, after fouling with humic acid. Seidel and Elimelech obtained a flux reduction up to 55% for an initial permeate flux up to 16.9 µm.s^{-1} [40].

Table 2 - Flux decline as a function of initial permeate flux

Initial Permeate Flux ($L.h^{-1}.m^{-2}$)	Operating pressure (bar)	Flux reduction (%)	Osmotic Backwashing flux ($L.h^{-1}.m^{-2}$)	PWF Recovery (%)
25	8	19 ± 4.2	13 ± 1	100 ± 2.3
50	14	49 ± 0.7	17 ± 2	90 ± 6.6
80	20	69 ± 1.4	16 ± 2	81 ± 7.5
100	30	75 ± 1.7	20 ± 2	70 ± 7.6

As can be seen in Figure 3, as the fouling layer thickness increases with increase in initial permeate flux, it becomes more challenging to remove. The fouling layer thickness on the membrane surface reduces by 77% for 25 $L.h^{-1}.m^{-2}$ (i.e. from 39 µm to 9 µm) and by 57% for 100 $L.h^{-1}.m^{-2}$ (i.e. from 270 µm to 115 µm). Organic fouling at higher pressures is largely irreversible due to the hydraulic pressure applied to the fouling layer, making it dense and compact [33]. The PWF recovery is directly proportional to the initial permeate flux. The PWF was more effectively restored at 100% for initial permeate fluxes of 25 $L.h^{-1}.m^{-2}$, reducing to 70% for 100 $L.h^{-1}.m^{-2}$ (Table 2). This happens despite an increase in osmotic backwashing flux with increased initial permeate flux. This could potentially be due to cake enhanced concentration polarization during fouling becoming more severe for higher fluxes [11, 46], and therefore due to the accumulation of ions on the membrane surface, causing a higher driving force for osmotic backwashing flux during cleaning.

The effects of pressure and initial permeate flux on fouling are evident when initial permeate fluxes of 50 and 80 $L.h^{-1}.m^{-2}$ are examined. The fouling layer thicknesses were similar, of 174 µm and 179 µm, respectively, and similar osmotic backwashing fluxes were obtained, of 17 $L.h^{-1}.m^{-2}$ and 16 $L.h^{-1}.m^{-2}$, respectively. However, osmotic backwashing is ineffective for an initial permeate flux of 80 $L.h^{-1}.m^{-2}$, as only 18% of the fouling layer was removed when compared to a 72% removal for 50 $L.h^{-1}.m^{-2}$. This was accompanied by a PWF restoration of 81% for 80 $L.h^{-1}.m^{-2}$ as opposed to a PWF restoration of 90% for 50 $L.h^{-1}.m^{-2}$. Although the fouling has the same thickness, the layer is denser and stronger for 80 $L.h^{-1}.m^{-2}$ due to the higher permeate drag applied by the higher hydraulic pressure. This is evident in Table 2, as a higher permeate flux decline of 49% vs 69% was obtained for 50 vs 80 $L.h^{-1}.m^{-2}$, respectively.

The osmotic backwashing flux generated with 0.7 M NaCl becomes inefficient for initial permeate fluxes higher than 50 $L.h^{-1}.m^{-2}$ for AA solutions with 2.5 mM Ca^{2+}, due to the

denser and more cohesive characteristics of the fouling. As the fouling is more difficult to remove, a higher osmotic backwashing flux is required in order to remove fouling layers developed under more challenging conditions.

3.3 Effect of backwashing flux on fouling removal of RO membranes

A way to improve cleaning efficiency is to increase the osmotic backwashing flux through the RO membrane by increasing the draw solution osmotic pressure. This can be achieved by either increasing the draw solution NaCl concentration or by using a different salt in the draw solution, e.g. $CaCl_2$. As such, draw solutions of 0.7 M and 4 M NaCl, as well as 3 M $CaCl_2$ were used for osmotic backwashing. These 3 ionic solutions originated osmotic pressures and backwashing fluxes shown in Table S1. Increasing the draw solution osmotic pressure increased the osmotic backwashing flux from 16 to 48 $L.h^{-1}.m^{-2}$, resulting in higher drag for more efficient fouling removal.

The osmotic pressure difference is the driving force and therefore as it increases, osmotic backwashing flux increases and more of the fouling layer would be expected to be removed. However, as can be seen in Figure 4, this is not the case. The initial fouling layer thickness was 179 µm. After osmotic backwashing, the remaining fouling layers range between 132 and 150 µm, despite an osmotic backwashing flux increase from 16 to 48 $L.h^{-1}.m^{-2}$. The low fouling removal with both NaCl draw solutions is surprising, as not only a higher osmotic backwashing flux with 4 M NaCl should enhance cleaning, but it has been hypothesized that Na^+ ions can exchange with Ca^{2+} within the AA layer, swelling it and contributing to a high cleaning efficiency [23]. In terms of PWF restoration, osmotic backwashing with 0.7 M and 4 M NaCl restored 81% and 86% of the PWF, respectively, despite the low removal of the fouling layer. This reinforces that flux restoration alone is not a sufficient indicator of efficient membrane cleaning and should ideally be accompanied by membrane surface observations. Surprisingly, when a draw solution of 3 M $CaCl_2$ was used, the PWF recovery was of 40% only, which is much lower compared to the NaCl draw solutions tested. This occurs despite a higher osmotic backwashing flux of 48 $L.h^{-1}.m^{-2}$ and a lower fouling thickness of 132 µm remaining on the membrane surface after cleaning.

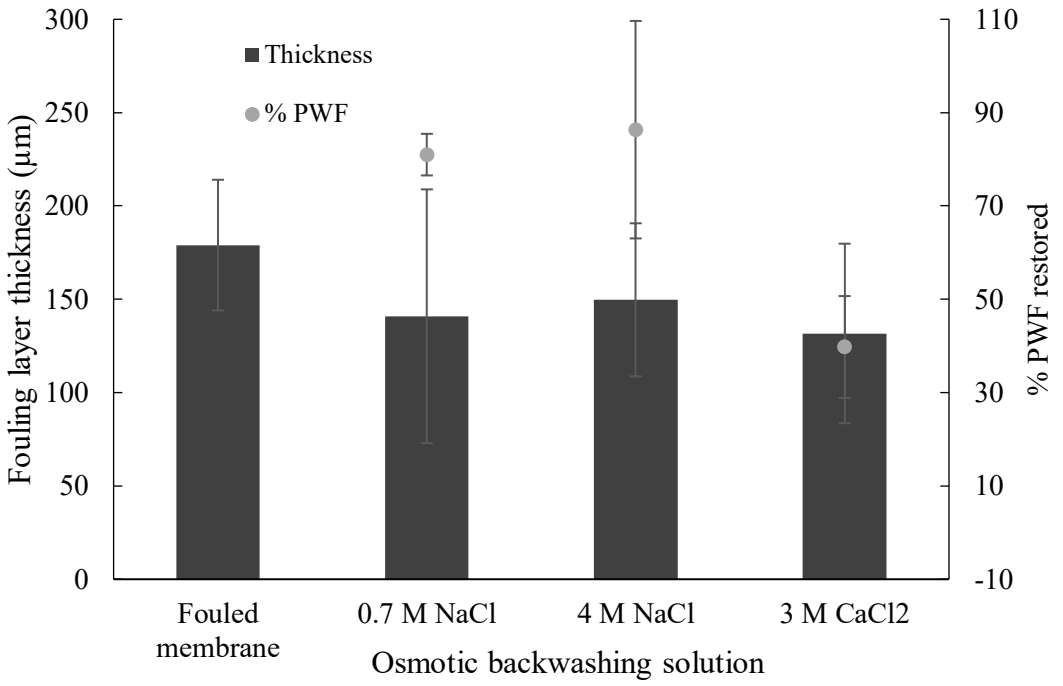

Figure 4 – Fouling thickness before and after osmotic backwashing and %PWF restored as a function of the osmotic backwashing solution (fouling conditions: FS = 60 mgC.L^{-1} AA, 1 mM $NaHCO_3$, 20 mM NaCl, 2.5 mM $CaCl_2$; initial permeate flux = 80 L.m^{-2}.h^{-1}; fouling duration = 6.5 hours; osmotic backwashing conditions: duration = 1 minute; error bars show standard deviation of repeated experiments)

The results in Figure 4 suggest that Ca^{2+} in the draw solution interferes with the fouling layer and forms complexes with the AA carboxylic groups. This makes it denser and more cohesive, despite only being exposed to Ca^{2+} for 1 minute. Mosta et al. [2] studied the relationship between alginate and Ca^{2+} ions in FO fouling and found that once the surface is covered with foulant, the fouling depends more on the foulant-foulant interactions than hydrodynamic conditions such as permeation drag. This could be a potential reason why $CaCl_2$ is not an effective osmotic backwashing solution, as the reversed permeate drag is not enough to overcome the strong adhesion forces caused by the interaction between the Ca^{2+} ions and the AA fouling layer. In order to further examine the interference of Ca^{2+} ions with the AA fouling layer during osmotic backwashing, a direct comparison between osmotic backwashing with $CaCl_2$ and NaCl was made.

3.4 Influence of type of salt used during BW of alginic acid fouled RO membranes

In order to directly compare between NaCl and $CaCl_2$ draw solutions, osmotic backwashing was carried out with NaCl and $CaCl_2$ draw solutions providing similar osmotic backwashing fluxes. In addition to visualizing the fouling layer thicknesses before osmotic backwashing, as well as after osmotic backwashing followed by PWF recovery testing, the membrane was also visualized immediately after osmotic backwashing, i.e. prior to measuring for PWF recovery. The fouling thicknesses obtained are shown in Figure 5. These samples were also characterised for adhesion forces and elasticity through Young's modulus determination by AFM (see Supporting Information Table S2), as well as visualized using a Cryo SEM (see Supporting Information Figure S1).

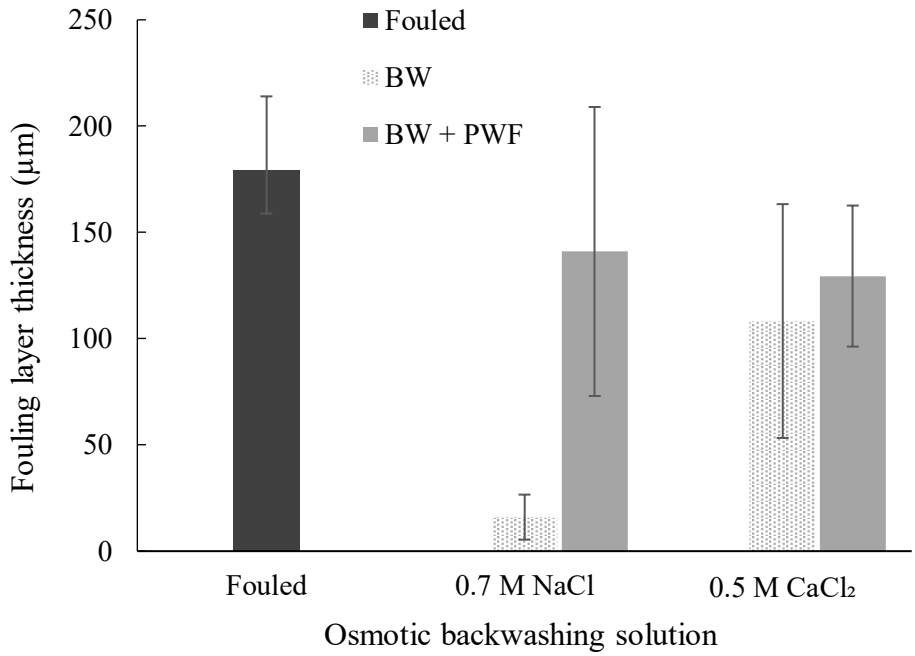

Figure 5 – Fouling thickness before osmotic backwashing, after osmotic backwashing (BW) and after osmotic backwashing and PWF measurement (BW+PWF) as a function of the osmotic backwashing solution (fouling conditions: FS = 60 $mgC.L^{-1}$ AA, 1 mM $NaHCO_3$, 20 mM NaCl, 2.5 mM $CaCl_2$; initial permeate flux = 80 $L.m^{-2}.h^{-1}$; fouling duration = 6.5 hours; osmotic backwashing conditions: duration = 1 minute; error bars show standard deviation of repeated experiments)

The membranes shown in Figure 5 were fouled under identical conditions and the draw solutions applied originated very similar osmotic backwashing fluxes, i.e. 16 ± 2.2 $L.h^{-1}.m^{-2}$ and 18 ± 0.4 $L.h^{-1}.m^{-2}$. The fouling thickness remaining after osmotic backwashing and PWF restoration measurements is slightly higher for 0.7 M NaCl, i.e. 141 µm, when compared to 0.5 M $CaCl_2$, i.e. 129 µm. As both membranes were cleaned with the same osmotic backwashing flux, this result is expected. However, cleaning with a 0.5 M $CaCl_2$ draw solution restored only 52% of the PWF, as opposed to 81% for 0.7 M NaCl. This result is surprising, as the membranes were fouled under the exact same conditions and both draw solutions originated similar osmotic backwashing fluxes and removed similar quantities of fouling (Figure 5). These results indicate that osmotic backwashing with different draw solutions can have an impact on the remaining fouling layer, changing its properties: the fouling subjected to a NaCl draw solution seems to offer less resistance to PWF when compared to the fouling subjected to a $CaCl_2$ draw solution. This is further evident when comparing osmotic backwashing between a 3 M $CaCl_2$ draw solution (Figure 4) with a 0.5 M $CaCl_2$ draw solution (Figure 5): 3 M $CaCl_2$ generated an osmotic backwashing flux of 48 $L.h^{-1}.m^{-2}$, with 132 µm of fouling left on the membrane and a PWF recovery of 40% as opposed to 0.5 M $CaCl_2$, which generated a lower osmotic backwashing flux of 18 $L.h^{-1}.m^{-2}$, leaving 129 µm of fouling on the membrane, but having a higher PWF recovery of 52%.

Fouling layer thicknesses were also observed for each draw solution tested immediately after osmotic backwashing was carried out, but prior to PWF testing. As can be seen in Figure 5, there are substantial differences in the characteristics of the fouling layers: after cleaning, the fouling layer thicknesses reduced from 179 µm to 16 µm using a draw solution of 0.7 M NaCl, and from 179 µm to 108 µm using a draw solution of 0.5 M $CaCl_2$. These differences can be further seen in the cryo-SEM images obtained. There is a stark contrast in appearance between the fouled membrane (Figure S1A) and the membrane osmotically backwashed with NaCl (Figure S1B): during osmotic backwashing the fouling layer reduces in thickness (see Figure 5), resulting in change in the fouling layer structure, which becomes flatter and more homogeneous. This is further confirmed using AFM to measure the elastic properties of the samples. The apparent Young's modulus for the virgin membrane and the fouled membrane show that the virgin membrane is stiff, with the highest apparent Young's modulus, i.e. 45270 kPa, whilst the fouled membrane is very soft and compliant, at 54 kPa. When osmotically backwashed with NaCl, a large part of the fouling is removed and the layer becomes thinner and more homogeneous (Figure S1B), translating to an apparent Young's modulus of 28475

kPa, hence more compliant than the virgin membrane, but stiffer than the fouled membrane (Table S2). This could be due to the fact that fouling layer sections close to the membrane surface are more compact than the layers above, as shown for biofouling [10].

When $CaCl_2$ is used in the draw solution, the Ca^{2+} ions interact with the AA layer, forming a more heterogeneous gel-like structure (Figure S1D). This is confirmed by the apparent Young's modulus, which shows a layer slightly stiffer than the fouled membrane at 112 kPa, but with more compliant characteristics when compared to 28475 kPa for a 0.7 M NaCl draw solution. Studies have previously demonstrated that crosslinking AA with Ca^{2+} was found to increase the elastic properties of biofilms [47, 48].

Adhesion force measurements (Table S2) further confirm a change in the characteristics of the fouling layers. The adhesion force of the fouled membrane was determined as 28 nN, increasing to 66 nN and 80 nN for the fouling remaining after cleaning with 0.7 M NaCl and 0.5 M $CaCl_2$ draw solutions, respectively. This is in line with other studies [10, 49] which showed an increase in the alginic acid adhesion forces with increase in Na^+ and Ca^{2+} concentrations, and higher adhesion forces obtained for Ca^{2+} when compared with Na^+. Higher adhesion forces in the presence of Ca^{2+} [10] hence reduce cleaning efficiency and PWF recovery (Figure 5).

When these remaining fouling layers are subjected to clean water for PWF recovery measurements, further changes in the fouling characteristics were noticed. The fouling layer subjected to 0.7 M NaCl swelled up to 9 times its thickness after the PWF test, whilst the fouling layer subjected to 0.5 M $CaCl_2$ swelled by only 1.2 times its thickness (Figure 5). This is further evidenced when comparing Cryo-SEM images: the fouling layer subjected to a NaCl draw solution becomes more porous and swollen in appearance after PWF testing, seen in Figures S1B and S1C. The apparent Young's modulus shows that the NaCl osmotically backwashed + PWF layer becomes very soft and flexible, i.e. 3046 kPa, as opposed to 28475 kPa before PWF testing. This contrasts with the fouling layer subjected to a $CaCl_2$ draw solution, whose morphology does not change to the same extent after PWF testing (Figures S1D and S1E), and showing no porous structure as the one exposed to a NaCl draw solution. The apparent Young's modulus shows again a negligible difference before and after PWF testing, i.e. 112 vs 114 kPa.

Swelling of alginate gels when the concentration of the surrounding monovalent ion solution is decreased has been previously discussed in other studies [31, 50]. Moe et al. [41]

explain that the swelling of the AA gel is due to both the osmotic pressure and elasticity of the gel. The gel has a high osmotic pressure due to its high ion concentration when exposed to high monovalent ion solutions (e.g. during osmotic backwashing). When this is followed by contact with solutions of lower ionic strength, i.e. lower osmotic pressure, such as deionized water, a driving force for water to enter the gel layer is established, thus causing it to swell. Moe et al. further show that alginate gels in divalent ion solutions like $CaCl_2$ shrink when the solution concentration is increased, but they exhibit hysteresis and do not re-swell when the concentration is decreased. Hence, swelling does not occur with draw solutions of $CaCl_2$. The swelling of the remaining fouling layer when cleaning with 0.7 M NaCl + PWF explains why the PWF recovery is higher for NaCl, i.e. 81%, than the PWF recovery obtained with $CaCl_2$, i.e. 52%, despite a slightly thinner fouling layer obtained for $CaCl_2$ after PWF measurement. Tow et al. [20] noted this swelling phenomenon when cleaning RO membranes of AA. In their study, they fouled RO membranes with AA, $CaCl_2$ and NaCl under pressure. During cleaning, the pressure was relieved, and wrinkling, swelling and eventual removal of the AA layer was noticed. They explain this is due to the gel having a high concentration of ions caused by cake enhanced concentration polarization during filtration at high pressure, followed by swelling of the AA layer due to the gel becoming in contact with lower concentrations of salt by simply relieving the pressure. This method resulted in a flux restoration of 80%.

The swelling of the fouling layer exposed to 0.7 M NaCl + PWF, strips the fouling layer of ions, and reduces the adhesion forces from 66 to 45 nN. Lower ionic strength has been shown to translate to lower AA adhesion forces [10, 49]. The same occurs for the layer exposed to 0.5 M $CaCl_2$ + PWF. However, the swelling is much less pronounced (Figure 5) and hysteresis occurs, hence not fully explaining why the adhesion forces reduce from 80 to 52 nN. A reduction in adhesion forces could be explained if the Ca^{2+} concentration in the fouling layer reduced [10, 49]. Each of the fouling layers on the membranes in Figure 5 were hence imaged by SEM-EDS (See Supporting Information Figure S2) and analysed for Ca^{2+} concentration, as shown in Table 3.

Table 2 – Apparent Ca^{2+} concentration for the different membrane samples

Membrane Sample	**Apparent Ca^{2+} Concentration**
Virgin	0
Fouled with AA and 2.5 mM $CaCl_2$	7.7 ± 0.5
BW with 0.7 M NaCl	6.2 ± 0.1
BW with 0.5 M $CaCl_2$	10.4 ± 0.6
BW with 0.7 M NaCl + PWF	0
BW with 0.5 M $CaCl_2$ + PWF	8.8 ± 0.3

Comparing the amount of Ca^{2+} on each membrane sample confirms that Ca^{2+} interacts with the fouling layer during osmotic backwashing. The virgin membrane contains no calcium (Figure S2a). The membrane fouled with AA and 2.5 mM of Ca^{2+} in the feed solution shows an apparent Ca^{2+} concentration of 7.7 due to the complexation between the AA molecules and the Ca^{2+} ions (Figure S2b). When this membrane was osmotically backwashed with 0.7 M NaCl, Ca^{2+} concentration decreased to 6.2, partly due to the removal of the fouling layer (Figure 5) and partly because of the ion exchange that occurs during osmotic backwashing between Na^{+} in the draw solution and Ca^{2+} in the fouling layer [23], as previously mentioned (Figure S1c where localised Cl^{-} is evident by blue patches). In contrast, after osmotic backwashing with 0.5 M $CaCl_2$, the apparent Ca^{2+} concentration increases to 10.4, further showing that Ca^{2+} interaction and binding occurs within the AA layer during osmotic backwashing (Figure S2E). The PWF testing phase further reduced the Ca^{2+} concentration in the fouling layer for both cases. Where NaCl was used as the draw solution, Ca^{2+} concentration was reduced to 0 (Figure S2D). This could be due to the 4-fold swelling of the AA layer (Figure 5) and a diffusion of the Ca^{2+} ions from the layer to the draw solution. The lack of Ca^{2+} ions in this layer explains why the layer is less cohesive and why PWF recovery is higher, i.e. 81%. Where $CaCl_2$ was used as the draw solution, a smaller reduction in Ca^{2+} concentration occurred, down to 8.8, as the bound Ca^{2+} ions are not released (Figure S2F), and the PWF recovery is lower, i.e. 52%. These results hence confirm a high degree of stripping of Ca^{2+} ions for 0.7 M NaCl + PWF, and less stripping for 0.5 M $CaCl_2$, hence explaining further why adhesion forces for these layers reduce (Table S2).

These results hence show that Ca^{2+} in the draw solution interferes negatively with the AA fouling layer, which also has shown a low swelling potential compared to AA fouling layers exposed to NaCl draw solutions. When monovalent salts are present in the draw solution, they diffuse into the fouling layer, increasing its ionic strength and hence, its osmotic pressure.

When the fouling layer is subsequently put in contact with a solution of low ionic strength, hence low osmotic pressure, the difference in osmotic pressure between the solution and the fouling layer causes water to penetrate the fouling layer, thus causing it to swell. The solution of low ionic strength concentration could be freshwater, wastewater reuse or brackish water of low salinity, depending what the membrane process is treating.

3.5 Influence of type of salt used during BW of organic fouled RO membranes

As the AA layer was found to change its characteristics when exposed to different salt solutions of different concentrations during osmotic backwashing and PWF recovery measurements, the same experiments in section 3.4 were carried out with other types of organic matter, i.e. humic acid (HA) and bovine serum albumin (BSA). The results are presented in Figure 6.

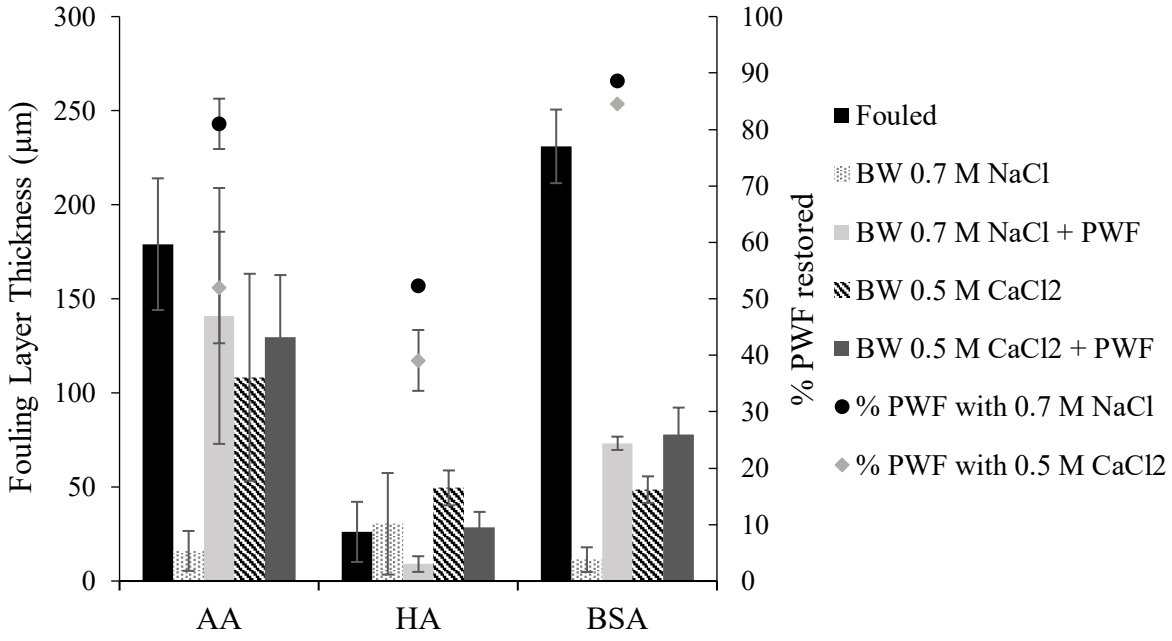

Figure 6 - Fouling thickness before osmotic backwashing, after osmotic backwashing (BW) and after osmotic backwashing and PWF measurement (BW+PWF) as a function of the osmotic backwashing solution and for different types of foulants (fouling conditions: FS = 60 mgC.L^{-1} of foulant, 1 mM $NaHCO_3$, 20 mM NaCl, 2.5 mM $CaCl_2$; initial permeate flux = 80 L.m^{-2}.h^{-1}; fouling duration = 6.5 hours; osmotic backwashing conditions: duration = 1 minute; error bars show standard deviation of repeated experiments)

As can be seen in Figure 6, the BSA fouling layer followed the same trend as AA when osmotic backwashing was carried out with NaCl and $CaCl_2$. Cleaning with 0.7 M NaCl, which produced an osmotic backwashing flux of 19 $L.h^{-1}.m^{-2}$, reduced the fouling layer thickness from 231 μm to 12 μm, hence a 95% reduction. After testing for PWF recovery, the fouling layer swelled up to 73 μm, resulting in an increase in thickness of 609%. The PWF recovery was of 89%, showing that despite an increase in thickness due to the swelling, hydraulic resistance of the fouling layer was low and PWF recovery was high, as similarly obtained for AA. In contrast, after osmotic backwashing with 0.5 M $CaCl_2$, which originated an osmotic backwashing flux of 21 $L.h^{-1}.m^{-2}$, more fouling remained on the membrane, with a thickness of 49 μm, hence only a 79% reduction was obtained when compared to 95% with NaCl cleaning. After exposing the remaining fouling layer to PWF recovery testing, swelling occurs, but to a much lesser extent, with an increase in thickness from 49 μm to 78 μm. The PWF recovery was slightly lower as well, of 84%. However, the interaction between calcium and BSA has been shown to be less pronounced when compared to AA and HA [37], hence why PWF recoveries for BSA are similar and why cleaning by osmotic backwashing is more efficient using a $CaCl_2$ draw solution.

In regards to fouling behaviour, HA did not follow the same trends as AA and BSA. In fact, the HA layer seems to swell slightly after osmotic backwashing with 0.7 NaCl and 0.5 M $CaCl_2$, increasing from 26 μm to 30 μm and 50 μm, respectively. When PWF recovery was measured, the thicknesses reduced to 9 μm for the layer exposed to 0.7 NaCl and 29 μm for the layer exposed to 0.5 M $CaCl_2$. The PWF recovery values obtained, however, follow the same trend as the other organic matter, in that PWF recovery with 0.7 M NaCl osmotic backwashing was higher, of 52%, as opposed to 39% for osmotic backwashing with 0.5 M $CaCl_2$. This shows that the presence of Ca^{2+} in the draw solution causes a similar effect on HA as it does on BSA and AA, forming more cohesive layers that are more difficult to remove.

Conclusion

Osmotic backwashing with a 0.7 M NaCl draw solution, i.e. concentrations similar to seawater, achieved good cleaning results, with obtained PWF recoveries higher than 90% and with less than 25 μm of fouling layer thickness left on the membrane for initial permeate fluxes up to 50 $L.h^{-1}.m^{-2}$ and in the presence of 2.5 mM $CaCl_2$ in the feed solution. However, with increasing initial permeate fluxes during fouling, the fouling layer became too compact and cohesive, and cleaning efficiency reduced. Increasing the osmotic backwashing flux could

potentially solve this. However, interactions between the salts in the osmotic backwashing solution and the fouling layer occurred, affecting cleaning efficiency.

Osmotic backwashing with monovalent salts followed by filtration of a solution of lower ionic strength than the one used as a draw solution, causes water to penetrate the fouling layer, thus swelling it. This was shown to happen with AA gels, and other foulants that are also hygroscopic, i.e. they can hold several times their weight in water, like BSA and HA. This swollen and hydrated layer offers little hydraulic resistance to water permeation, hence why PWF recoveries are high. However, this does not occur when the fouling layers are exposed to divalent draw solutions like $CaCl_2$, as little to no swelling is obtained. In fact, the Ca^{2+} interacts with the organic fouling layer, making it more cohesive and increasing adhesion forces, and therefore, making it more difficult to remove. Once they are exposed to solutions of low ionic strength, they exhibit hysteresis and do not swell up. This denser and more compact fouling layer hence presents higher hydraulic resistance to permeation, and PWF recoveries are lower. Despite offering higher osmotic backwashing fluxes, Ca^{2+} based salts should not be used for osmotic backwashing of organic fouled RO membranes, and other avenues to increase osmotic backwashing fluxes need to be researched, such as by starting osmotic backwashing at a higher pressure to enhance concentration polarisation, followed by lowering the hydraulic applied pressure, and hence starting the cleaning at a higher osmotic pressure difference between the feed and permeate sides.

Acknowledgements

The authors would like to thank the School of Engineering at the University of Edinburgh for the PhD studentship awarded to Dr. Sorcha Daly and the start-up funds awarded to Dr. Andrea Semião, as well as thank EPSRC funding (EP/P021646/1). The authors would like to acknowledge the invaluable help and input from the School of Engineering Workshop in the redesign and construction of the RO membrane setup. The authors would like to thank Dr. David Kelly from the Centre Optical Instrumentation Laboratory (COIL) for all his help with the fluorescent microscopy and Dr. Nicola Cayzer for all her help with the SEM-EDS and mapping at the Grant Institute, School of GeoSciences at the University of Edinburgh. Finally the authors would like to thank Steve Mitchell and Dr. Kathryn Topham at the School of Biological Sciences at the University of Edinburgh for their help with the Cryo-SEM.

1. Service, R.F., *Desalination Freshens Up.* Science, 2006. **313**(5790): p. 1088-1090.DOI: 10.1126/science.313.5790.1088.
2. Motsa, M.M., et al., *Organic fouling in forward osmosis membranes: The role of feed solution chemistry and membrane structural properties.* Journal of Membrane Science, 2014. **460**(0): p. 99-109.DOI: http://dx.doi.org/10.1016/j.memsci.2014.02.035.
3. Ghaffour, N., T.M. Missimer, and G.L. Amy, *Technical review and evaluation of the economics of water desalination: Current and future challenges for better water supply sustainability.* Desalination, 2013. **309**: p. 197-207.DOI: https://doi.org/10.1016/j.desal.2012.10.015.
4. Flemming, H.-C., et al., *Effects and extent of biofilm accumulation in membrane systems*, in *Biofouling and Biocorrosion in Industrial Water Systems*, G.G. Geesey, Z. Lewandowski, and H.-C. Flemming, Editors. 1994, CRC Press, USA. p. 63-105.
5. Greenlee, L.F., et al., *Reverse osmosis desalination: Water sources, technology, and today's challenges.* Water Research, 2009. **43**(9): p. 2317-2348.DOI: http://dx.doi.org/10.1016/j.watres.2009.03.010.
6. Tang, C.Y., Y.-N. Kwon, and J.O. Leckie, *Fouling of reverse osmosis and nanofiltration membranes by humic acid—Effects of solution composition and hydrodynamic conditions.* Journal of Membrane Science, 2007. **290**(1–2): p. 86-94.DOI: http://dx.doi.org/10.1016/j.memsci.2006.12.017.
7. Tang, C.Y., Y.-N. Kwon, and J.O. Leckie, *Characterization of Humic Acid Fouled Reverse Osmosis and Nanofiltration Membranes by Transmission Electron Microscopy and Streaming Potential Measurements.* Environmental Science & Technology, 2007. **41**(3): p. 942-949.DOI: 10.1021/es061322r.
8. Xie, M., et al., *Comparison of the removal of hydrophobic trace organic contaminants by forward osmosis and reverse osmosis.* Water Research, 2012. **46**(8): p. 2683-2692.DOI: http://dx.doi.org/10.1016/j.watres.2012.02.023.
9. Ying, W., et al., *New insights on early stages of RO membranes fouling during tertiary wastewater desalination.* Journal of Membrane Science, 2014. **466**(0): p. 26-35.DOI: http://dx.doi.org/10.1016/j.memsci.2014.04.027.
10. Lee, S. and M. Elimelech, *Relating Organic Fouling of Reverse Osmosis Membranes to Intermolecular Adhesion Forces.* Environmental Science & Technology, 2006. **40**(3): p. 980-987.DOI: 10.1021/es051825h.
11. Herzberg, M. and M. Elimelech, *Biofouling of reverse osmosis membranes: Role of biofilm-enhanced osmotic pressure.* Journal of Membrane Science, 2007. **295**(1): p. 11-20.DOI: https://doi.org/10.1016/j.memsci.2007.02.024.
12. Ang, W.S., et al., *Chemical cleaning of RO membranes fouled by wastewater effluent: Achieving higher efficiency with dual-step cleaning.* Journal of Membrane Science, 2011. **382**(1–2): p. 100-106.DOI: http://dx.doi.org/10.1016/j.memsci.2011.07.047.
13. Ang, W.S., et al., *Fouling and cleaning of RO membranes fouled by mixtures of organic foulants simulating wastewater effluent.* Journal of Membrane Science, 2011. **376**(1–2): p. 196-206.DOI: http://dx.doi.org/10.1016/j.memsci.2011.04.020.
14. Lattemann, S. and T. Höpner, *Environmental impact and impact assessment of seawater desalination.* Desalination, 2008. **220**(1–3): p. 1-15.DOI: http://dx.doi.org/10.1016/j.desal.2007.03.009.
15. Simon, A., et al., *Effects of membrane degradation on the removal of pharmaceutically active compounds (PhACs) by NF/RO filtration processes.* Journal of Membrane Science, 2009. **340**(1): p. 16-25.DOI: https://doi.org/10.1016/j.memsci.2009.05.005.
16. Klüpfel, A.M. and F.H. Frimmel, *Nanofiltration of river water — fouling, cleaning and micropollutant rejection.* Desalination, 2010. **250**(3): p. 1005-1007.DOI: https://doi.org/10.1016/j.desal.2009.09.091.

17. Bar-Zeev, E. and M. Elimelech, *Reverse Osmosis Biofilm Dispersal by Osmotic Back-Flushing: Cleaning via Substratum Perforation.* Environmental Science & Technology Letters, 2014. **1**(2): p. 162-166.DOI: 10.1021/ez400183d.
18. Lee, S., et al., *Comparison of fouling behavior in forward osmosis (FO) and reverse osmosis (RO).* Journal of Membrane Science, 2010. **365**(1–2): p. 34-39.DOI: http://dx.doi.org/10.1016/j.memsci.2010.08.036.
19. Ramon, G.Z., T.-V. Nguyen, and E.M.V. Hoek, *Osmosis-assisted cleaning of organic-fouled seawater RO membranes.* Chemical Engineering Journal, 2013. **218**(0): p. 173-182.DOI: http://dx.doi.org/10.1016/j.cej.2012.12.006.
20. Tow, E.W., M.M. Rencken, and J.H. Lienhard, *In situ visualization of organic fouling and cleaning mechanisms in reverse osmosis and forward osmosis.* Desalination, 2016. **399**: p. 138-147.DOI: https://doi.org/10.1016/j.desal.2016.08.024.
21. Qin, J.-J., et al., *Development of novel backwash cleaning technique for reverse osmosis in reclamation of secondary effluent.* Journal of Membrane Science, 2010. **346**(1): p. 8-14.DOI: http://dx.doi.org/10.1016/j.memsci.2009.08.011.
22. Qin, J.-J., B. Liberman, and K. Kekre, *Direct Osmosis for Reverse Osmosis Fouling Control: Principles, Applications and Recent Developments.* The Open Chemical Engineering Journal, 2009. **3**: p. 8-16.DOI: 10.2174/1874123100903010008.
23. Lee, S. and M. Elimelech, *Salt cleaning of organic-fouled reverse osmosis membranes.* Water Research, 2007. **41**(5): p. 1134-1142.DOI: http://dx.doi.org/10.1016/j.watres.2006.11.043.
24. Jiang, W., et al., *An innovative backwash cleaning technique for NF membrane in groundwater desalination: Fouling reversibility and cleaning without chemical detergent.* Desalination, 2015. **359**: p. 26-36.DOI: https://doi.org/10.1016/j.desal.2014.12.025.
25. Nam, J.W., et al., *Effect on backwash cleaning efficiency with TDS concentrations of circulated water and backwashing water in SWRO membrane.* Desalination and Water Treatment, 2012. **43**(1-3): p. 124-130.DOI: 10.1080/19443994.2012.672162.
26. Sagiv, A., et al., *Osmotic backwash mechanism of reverse osmosis membranes.* Journal of Membrane Science, 2008. **322**(1): p. 225-233.DOI: http://dx.doi.org/10.1016/j.memsci.2008.05.055.
27. Sagiv, A. and R. Semiat, *Parameters affecting backwash variables of RO membranes.* Desalination, 2010. **261**(3): p. 347-353.DOI: http://dx.doi.org/10.1016/j.desal.2010.04.012.
28. Daly, S. and A.J.C. Semiao, *Mechanisms Involved in Osmotic Backwashing of Fouled Forward Osmosis (FO) Membranes.* Journal of Membrane Science and Research, 2020. **6**(2): p. 158-167.DOI: 10.22079/jmsr.2020.118843.1315.
29. Boo, C., et al., *Colloidal fouling in forward osmosis: Role of reverse salt diffusion.* Journal of Membrane Science, 2012. **390–391**(0): p. 277-284.DOI: http://dx.doi.org/10.1016/j.memsci.2011.12.001.
30. Ang, W.S., S. Lee, and M. Elimelech, *Chemical and physical aspects of cleaning of organic-fouled reverse osmosis membranes.* Journal of Membrane Science, 2006. **272**(1): p. 198-210.DOI: https://doi.org/10.1016/j.memsci.2005.07.035.
31. de Kerchove, A.J. and M. Elimelech, *Formation of Polysaccharide Gel Layers in the Presence of Ca2+ and K+ Ions: Measurements and Mechanisms.* Biomacromolecules, 2007. **8**(1): p. 113-121.DOI: 10.1021/bm060670i.
32. Mi, B. and M. Elimelech, *Organic fouling of forward osmosis membranes: Fouling reversibility and cleaning without chemical reagents.* Journal of Membrane Science, 2010. **348**(1–2): p. 337-345.DOI: http://dx.doi.org/10.1016/j.memsci.2009.11.021.
33. Xie, M., et al., *Role of pressure in organic fouling in forward osmosis and reverse osmosis.* Journal of Membrane Science, 2015. **493**: p. 748-754.DOI: https://doi.org/10.1016/j.memsci.2015.07.033.
34. Vu, B., et al., *Bacterial extracellular polysaccharides involved in biofilm formation.* Molecules (Basel, Switzerland), 2009. **14**(7): p. 2535-2554.DOI: 10.3390/molecules14072535.

35. Chang, W.-S., et al., *Alginate Production by Pseudomonas putida Creates a Hydrated Microenvironment and Contributes to Biofilm Architecture and Stress Tolerance under Water-Limiting Conditions.* Journal of Bacteriology, 2007. **189**(22): p. 8290.DOI: 10.1128/JB.00727-07.
36. Kim, Y., et al., *Combined organic and colloidal fouling in forward osmosis: Fouling reversibility and the role of applied pressure.* Journal of Membrane Science, 2014. **460**(0): p. 206-212.DOI: http://dx.doi.org/10.1016/j.memsci.2014.02.038.
37. Mi, B. and M. Elimelech, *Chemical and physical aspects of organic fouling of forward osmosis membranes.* Journal of Membrane Science, 2008. **320**(1–2): p. 292-302.DOI: http://dx.doi.org/10.1016/j.memsci.2008.04.036.
38. Hong, S. and M. Elimelech, *Chemical and physical aspects of natural organic matter (NOM) fouling of nanofiltration membranes.* Journal of Membrane Science, 1997. **132**(2): p. 159-181.DOI: https://doi.org/10.1016/S0376-7388(97)00060-4.
39. Li, Q. and M. Elimelech, *Organic Fouling and Chemical Cleaning of Nanofiltration Membranes: Measurements and Mechanisms.* Environmental Science & Technology, 2004. **38**(17): p. 4683-4693.DOI: 10.1021/es0354162.
40. Seidel, A. and M. Elimelech, *Coupling between chemical and physical interactions in natural organic matter (NOM) fouling of nanofiltration membranes: implications for fouling control.* Journal of Membrane Science, 2002. **203**(1): p. 245-255.DOI: https://doi.org/10.1016/S0376-7388(02)00013-3.
41. Moe, S.T., et al., *Swelling of covalently crosslinked alginate gels: influence of ionic solutes and nonpolar solvents.* Macromolecules, 1993. **26**(14): p. 3589-3597.DOI: 10.1021/ma00066a017.
42. Tang, C.Y., et al., *Effect of flux (transmembrane pressure) and membrane properties on fouling and rejection of reverse osmosis and nanofiltration membranes treating perfluorooctane sulfonate containing wastewater.* Environmental Science & Technology, 2007. **41**(6): p. 2008-2014.
43. Tang, C.Y., Y.-N. Kwon, and J.O. Leckie, *Fouling of reverse osmosis and nanofiltration membranes by humic acid—Effects of solution composition and hydrodynamic conditions.* Journal of Membrane Science, 2007. **290**(1): p. 86-94.DOI: https://doi.org/10.1016/j.memsci.2006.12.017.
44. Wang, Y.-N. and C.Y. Tang, *Nanofiltration Membrane Fouling by Oppositely Charged Macromolecules: Investigation on Flux Behavior, Foulant Mass Deposition, and Solute Rejection.* Environmental Science & Technology, 2011. **45**(20): p. 8941-8947.DOI: 10.1021/es202709r.
45. Lee, S., W.S. Ang, and M. Elimelech, *Fouling of reverse osmosis membranes by hydrophilic organic matter: implications for water reuse.* Desalination, 2006. **187**(1): p. 313-321.DOI: https://doi.org/10.1016/j.desal.2005.04.090.
46. Hoek, E.M.V. and M. Elimelech, *Cake-Enhanced Concentration Polarization: A New Fouling Mechanism for Salt-Rejecting Membranes.* Environmental Science & Technology, 2003. **37**(24): p. 5581-5588.DOI: 10.1021/es0262636.
47. Körstgens, V., et al., *Influence of calcium ions on the mechanical properties of a model biofilm of mucoid Pseudomonas aeruginosa.* Water Science and Technology, 2001. **43**(6): p. 49-57.DOI: 10.2166/wst.2001.0338.
48. Safari, A., et al., *The significance of calcium ions on Pseudomonas fluorescens biofilms – a structural and mechanical study.* Biofouling, 2014. **30**(7): p. 859-869.DOI: 10.1080/08927014.2014.938648.
49. Tang, C.Y., Y.-N. Kwon, and J.O. Leckie, *The role of foulant–foulant electrostatic interaction on limiting flux for RO and NF membranes during humic acid fouling—Theoretical basis, experimental evidence, and AFM interaction force measurement.* Journal of Membrane Science, 2009. **326**(2): p. 526-532.DOI: https://doi.org/10.1016/j.memsci.2008.10.043.

50. de Kerchove, A.J. and M. Elimelech, *Structural Growth and Viscoelastic Properties of Adsorbed Alginate Layers in Monovalent and Divalent Salts.* Macromolecules, 2006. **39**(19): p. 6558-6564.DOI: 10.1021/ma0527606.
51. Gysel, M., et al., *Hygroscopic properties of water-soluble matter and humic-like organics in atmospheric fine aerosol.* Atmos. Chem. Phys., 2004. **4**(1): p. 35-50.DOI: 10.5194/acp-4-35-2004.
52. Mikhailov, E., et al., *Interaction of aerosol particles composed of protein and saltswith water vapor: hygroscopic growth and microstructural rearrangement.* Atmos. Chem. Phys., 2004. **4**(2): p. 323-350.DOI: 10.5194/acp-4-323-2004.
53. Kallenberger, P.A. and M. Fröba, *Water harvesting from air with a hygroscopic salt in a hydrogel–derived matrix.* Communications Chemistry, 2018. **1**(1): p. 28.DOI: 10.1038/s42004-018-0028-9.